Supporting Information for:

Fluorescence Monitoring of Peptide Transport Pathways into Large and Giant Vesicles by Supramolecular Host-Dye Reporter Pairs

Andrea Barba-Bon, Yu-Chen Pan, Frank Biedermann, Dong-Sheng Guo, Werner M. Nau, and Andreas Hennig

Table of Contents

1 Materials S2
2 Abbreviations S3
3 Supramolecular Tandem Membrane Assays S3
3.1 CX4/LCG Assay S3
3.2 CB7/BE Assay S4
3.3 CB8/MDAP Assay S6
4 Macrocycles-Dye/Peptide Interactions S8
5 Silently–Translocating Peptide S10
6 Identification of Counterion Activators S10
7 Influence of Different Reporter Pairs S13
7.1 Solution Experiments S13
7.1.1 Binding of Peptides P2-P7 to CX4-H S13
7.1.2 Binding of Peptides P2-P7 2to Curcurbit[7]uril S14
7.1.3 Binding of Peptides P2-P7 to Curcurbit[8]uril/MDAP S15
7.1.4 Binding of Peptides P2-P7 to CX4-C5 ..... S16
7.2 Membrane Transport Experiments S17
7.2.1 CX4/LGC Assay S17
7.2.2 CB7/BE Assay S19
7.2.3 CB8/MDAP Assay S20
8 Transport in GUVs S22
8.1 CB8/MDAP Assay S22
8.1.1 Peptide Activation with Fluorophiles S22
8.1.2 Peptide Activation with CX4-C5 ..... S23
8.2 CX4/LCG Assay S25
8.2.1 Previously Silently Translocating Peptide S25
8.2.2 Heptaarginine Activation with CX4-C5 ..... S26
8.2.3 LCG Photobleaching S26
9 References S27

1 Materials

Materials. Reagents and compounds for buffer preparation and analytical measurements including 1-adamantylamine, berberine (BE), *p*-sulfonatocalix[4]arene sodium salt (CX4-H), lucigenin (LCG), perfluorooctanoic acid (F1), tricosafluorododecanoic acid (F2), 4,4,5,5,6,6,7,7,8,8,9,9,9-tridecafluorononanoic acid (F3), and 4,4,5,5,6,6,7,7,8,8,9,9,10,10,11,11,11-heptadecafluoroundecanoic acid (F4) were from Sigma-Aldrich (Steinheim, Germany). Heptaarginine (heptaArg) was from Bachem (Bubendorf, Switzerland), and egg yolk phosphatidylcholine (EYPC), 1-palmitoyl-2-oleoyl-s*n*-glycero-3-phosphocholine (POPC) and 1-palmitoyl-2-oleoyl-s*n*-glycero-3-[phosphor-L-serine] (POPS) were from Avanti Polar Lipids (Alabaster, AL, USA). Cucurbit[7]uril and cucurbit[8]uril were from Strem Chemicals Int. (Massachusetts, United States). 2,7-dimethyldiazapyrenium (MDAP) was synthesized as reported.[S1] NAP-25 Columns Sephadex G-25 DNA grade were from GE Heathcare (Buckinghamshire, United Kingdom). Peptides P1 and P3-P6 were custom-made by GeneCust (Dudelange, Luxembourg), and P7 by Biosyntan (Berlin, Germany) and all obtained in >95% purity as confirmed by HPLC and MS by the supplier. The amphiphilic *p*-sulfonatocalix[4]arene CX4-C5 was synthesized as reported.[S2] Buffers were prepared from solid Hepes or sodium dihydrogen phosphate and the pH was adjusted by addition of NaOH. Peptide stock solutions were prepared in water and their concentration was determined using the extinction coefficient of tryptophan at 280 nm (ε = 5540 M^{-1} cm^{-1})[S3] and phenylalanine at 257 nm (ε = 195 M^{-1} cm^{-1}).[S4]

Instrumentation. Absorption measurements were performed with a Varian Cary 4000 spectrophotometer. Fluorescence was measured with either a Varian Eclipse or a Jasco FP-8500 spectrofluorometer equipped with temperature controllers (T = 25 ˚C). All spectroscopic measurements were performed in 0.5 ml and 3.5 ml quartz glass cuvettes from Hellma Analytics (Müllheim, Germany) and 3.5 ml polymethylmethacrylate (PMMA) cuvettes from Sigma-Aldrich (Steinheim, Germany). Dynamic light scattering (DLS) experiments were carried out on a Malvern Instruments DTS Nano 2000 Zeta-Sizer. GUVs were observed with a Zeiss Axiovert 200 equipped with a digital camera (Evolution QEi Media Cybernetics).

2 Abbreviations

BE: berberine, CB7: cucurbit[7]uril, CB8: cucurbit[8]uril, CPPs: cell-penetrating peptides, CX4-C5: *p*-sulfonatocalix[4]arene tetrapentyl ether, CX4-H: *p*-sulfonatocalix[4]arene, GUV: giant unilamellar vesicle, DLS: dynamic light scattering, heptaArg: heptaarginine, LCG: lucigenin, LUV: large unilamellar vesicle, MDAP: 2,7-dimethyldiazapyrenium, POPC: 1-palmitoyl-2-oleoyl-s*n*-glycero-3-phosphocholine, POPS: 1-palmitoyl-2-oleoyl-s*n*-glycero-3-[phosphor-L-serine], TX-100: triton X-100.

3 Supramolecular Tandem Membrane Assays

3.1 CX4/LCG Assay

The principle of monitoring peptide uptake into vesicles by means of an encapsulated CX4/LCG reporter pair is shown in Scheme S1. Experimentally, 100 µL 25 mg/mL POPC in $CHCl_3$ was purged with nitrogen and dried *in vacuo* overnight. The lipid film was rehydrated with 1 mL 10 mM Hepes, 700 µM CX4 and 500 µM LCG, pH 7.0 by agitation at room temperature for 30 min. Then, the suspension was subjected to 15 freeze-thaw cycles. Extravesicular components were removed by size exclusion chromatography (NAP-25 column) with 10 mM Hepes, pH 7.0 to afford POPC⊃CX4/LCG liposome stock solutions. The vesicle size was confirmed by DLS and the phospholipid concentration was determined by the Stewart and NMR assays.[S5] In all experiments, the POPC⊃CX4/LCG liposome stock solution was diluted with 10 mM Hepes, pH 7.0 (final concentration, 12 µM phospholipids) in a disposable plastic cuvette and the time-dependent change in fluorescence intensity, I_t, was monitored (λ_{exc} = 369 nm, λ_{em} = 502 nm).

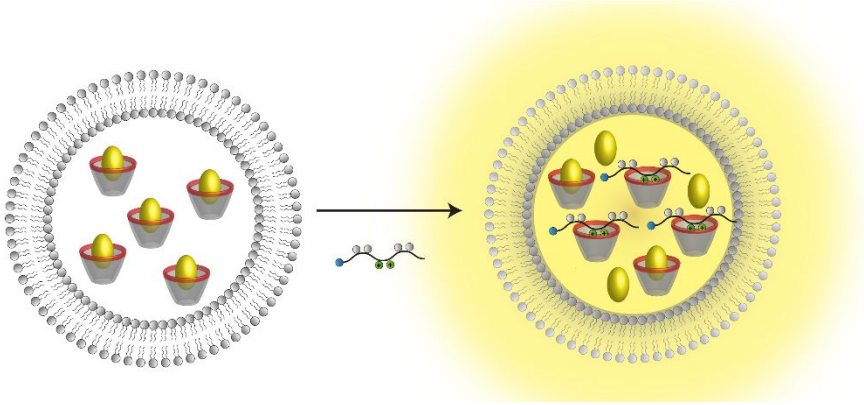

Scheme S1. Principle of supramolecular tandem membrane assay with CX4/LCG reporter pair.

The absence of reporter pair in the extravesicular phase was verified by adding spermine (as a non-permeable CX4 guest), and no significant change in fluorescence intensity upon addition of spermine verified the complete removal of unencapsulated CX4/LCG. For transport assays, counterion activator was added at t = 60 s (no counterion was added in the transport experiments with P1) and peptide at t = 120 s. At the end of the experiment, 24 µl 1.2 % (wt/vol) triton X-100 in water was added to lyse the vesicles for calibration. Time courses of I_t were normalized to fractional intensities, I_f, using the equation $I_f = (I_t - I_0) / (I_\infty - I_0)$, where I_0 = I_t before peptide addition and $I_\infty = I_t$ after lysis. For Hill analysis, I_f before lysis was defined as transmembrane activity, Y, and plotted against concentration counterion activator (or peptides), c, and fitted to the Hill equation (1) to afford the transmembrane activity in absence of peptide, Y_0, the maximal transmembrane activity, EC_{50}, and the Hill coefficient, n.

$$Y = Y_0 + \frac{(Y_{\max} - Y_0)}{1 + \left(\frac{EC_{50}}{c}\right)^n} \qquad (1)$$

3.2 CB7/BE Assay

The principle of monitoring peptide uptake into vesicles by means of an encapsulated CB7/BE reporter pair is shown in Scheme S2. To prepare the liposomes, 100 µL 25 mg/mL POPC and 33 µL 10 mg/mL POPS in $CHCl_3$ were purged with nitrogen and dried *in vacuo* overnight. The lipid film was rehydrated with 1 mL 10 mM $(NH_4)_2HPO_4$, 300 µM CB7, 500 µM BE, pH 7.0 and agitation at room temperature for 30 min. Then, the resulting suspension was subjected to 20 freeze-thaw cycles. Extravesicular components were removed by size exclusion chromatography (NAP-25 column) with 10 mM $(NH_4)_2HPO_4$, pH 7.0 to give POPC/POPS⊃CB7/BE liposome stock solutions. The vesicle size was confirmed by DLS and the phospholipid concentration was determined by the Stewart and NMR assays.[S5] In all experiments, the POPC/POPS⊃CB7/BE liposomes stock solution was diluted with 10 mM $(NH_4)_2HPO_4$, pH 7.0 (final concentration, 12 µM phospholipids) in a disposable plastic cuvette and the time-dependent change in fluorescence intensity, I_t, was monitored (λ_{exc} = 420 nm, λ_{em} = 495 nm).

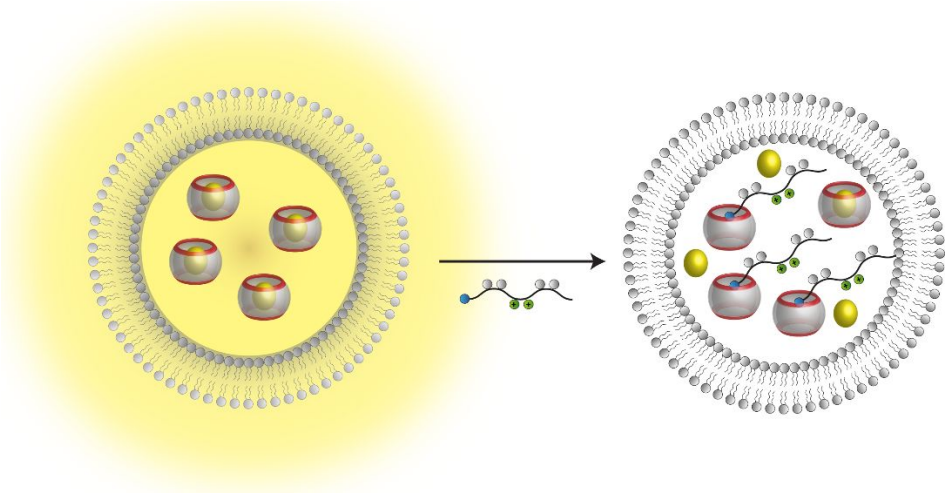

Scheme S2. Principle of supramolecular tandem membrane assay with CB7/BE reporter pair.

The absence of reporter pair in the extravesicular phase was verified by adding cadaverine (as a non-permeable CB7 guest), and a constant fluorescence intensity upon addition of cadaverine verified the removal of unencasulated CB7/BE. For transport assays, counterion activator was added at t = 60 s and peptide at t = 120 s; at the end of the experiment, 25 µM adamantylamine (as a membrane-permeable CB7 guest) was added for calibration. Time courses of I_t were normalized to fractional intensities, I_f, using the equation $I_f = (I_t - I_\infty) / (I_0 - I_\infty)$, where $I_0 = I_t$ at activator addition and $I_\infty = I_t$ at saturation after addition of adamantylamine. Since adamantylamine was used for calibration, which is known as a membrane-permeable, quantitative (K_a > 10^{10} M^{-1}) CB7 binder,[S6] I_f, just before addition of adamantylamine, can be converted into % displacement via eq (2), in which $I_{f,100\%}$ is I_f after addition of adamantylamine and $I_{f,0\%}$ is I_f in absence of membrane transporters just before addition of adamantylamine.

$$\%\ \text{displacement} = 100 \times {(I_f - I_{f,0\%})}/{(I_{f,100\%} - I_{f,0\%})} \qquad (2)$$

We postulate that I_f after addition of adamantylamine refers to 100% displacement and I_f in absence of membrane transporters just before addition of adamantylamine to 0% displacement. For Hill analysis, the % displacement values were plotted against the concentration of peptides, c, and fitted to the modified Hill equation (3) to afford the maximal % displacement with excess peptide, D_{max}, the concentration needed to achieve 50% of D_{max}, EC_{50}, and the Hill coefficient, n.

$$\%\ \text{displacement} = \frac{D_{\max}}{1 + \left(\frac{EC_{50}}{c}\right)^n} \qquad (3)$$

3.3 CB8/MDAP Assay

The principle of monitoring peptide uptake into vesicles by means of an encapsulated CB7/BE reporter pair is shown in Scheme S3. In detail, 100 µL 25 mg/mL POPC and 33 µL 10 mg/mL POPS in $CHCl_3$ were purged with nitrogen and dried *in vacuo* overnight. The lipid film was rehydrated with 1 mL 10 mM Hepes, 500 µM CB8, 550 µM MDAP, pH 7.0 and agitation at room temperature for 30 min. Then, the resulting suspension was subjected to 20 freeze-thaw cycles. Extravesicular components were removed by size exclusion chromatography (NAP-25 column) with 10 mM Hepes, pH 7.0 to give POPC/POPS⊃CB8/MDAP liposome stock solutions. The vesicle size was confirmed by DLS and the phospholipid concentration was determined by the Stewart and NMR assays.[S5] In all experiments, the POPC/POPS⊃CB8/MDAP liposome stock solution was diluted with 10 mM Hepes, pH 7.0 (final concentration, 12 µM phospholipids) in a disposable plastic cuvette and the time-dependent change in fluorescence intensity, I_t, was monitored (λ_{exc} = 339 nm, λ_{em} = 424 nm).

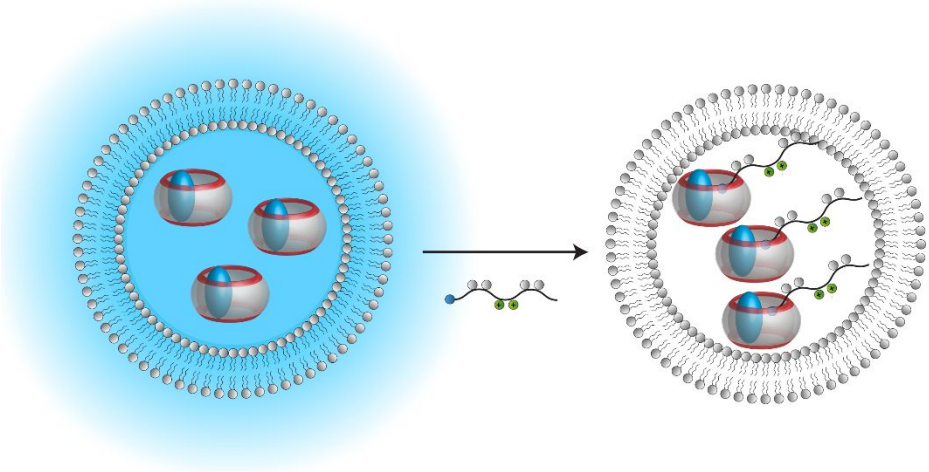

Scheme S3. Principle of supramolecular tandem membrane assay with CB8/MDAP reporter pair.

The absence of reporter pair in the extravesicular phase was verified by adding tryptophan (as non-permeable CB8 guest) and a negligible change in fluorescence intensity upon addition of tryptophan verified the removal of unencasulated CB8/MDAP. For transport assays, counterion activator was added at t = 60 s and peptide at t = 120 s; at the end of the experiment 25 µM tryptophan amide (as a membrane-permeable CB8 guest) was added for calibration. Time courses of I_t were normalized to fractional intensities, I_f, using the equation $I_f = (I_t - I_\infty) / (I_0 - I_\infty)$, where $I_0 = I_t$ at activator addition and $I_\infty = I_t$ at saturation after addition of tryptophan amide. Since tryptophan amide was used for calibration, I_f just before its addition

can be converted into % quenching efficiency, %QE, via eq (4) in which $I_{f,100\%}$ is I_f after addition of tryptophan amide and $I_{f,0\%}$ is I_f in absence of membrane transporters.

$$\%\mathrm{QE} = 100 \times {(I_\mathrm{f} - I_{\mathrm{f},0\%})}/{(I_{\mathrm{f},100\%} - I_{\mathrm{f},0\%})} \qquad (4)$$

Because tryptophan amide is a very efficient quencher of CB8/MDAP (data not shown), we postulate that I_f after addition of excess of tryptophan amide refers to 100% quenching efficiency and I_f in absence of membrane transporters to 0% quenching. For Hill analysis, the %QE values were plotted against the concentration of peptides, *c*, and fitted to the modified Hill equation (5) to afford the maximal quenching efficiency with excess of peptide, QE_{max}, the concentration needed to achieve 50% of QE_{max}, EC_{50}, and the Hill coefficient, *n*.

$$\%\mathrm{QE} = \frac{QE_{max}}{1 + \left(\frac{EC_{50}}{c}\right)^n} \qquad (5)$$

4 Macrocycles-Dye/Peptide Interactions

In order to determine the binding constants of the different peptides with the selected macrocycles (see Table S1) by competitive fluorescence titrations, we have chosen lucigenin (LCG) as fluorescent dye for CX4 and CX4-C5 and berberine (BE) for CB7, which bind strongly to the macrocycles[S7] and are membrane-impermeable.[S6] The respective examples of binding titrations are shown in Figures S1-S3.

Table S1: Binding constants, K_a, of dyes and peptides to the different macrocycles.

Guest	K_a (10^5 M^{-1})			
	CX4[a]	**CX4-C5**[a]	**CB7**[b]	**CB8**[a]
LCG	102 ± 15	22.1 ± 2.7	n.b.[c]	n.d.[d]
BE	n.b.[c]	n.b.[c]	13.2 ± 0.6	n.d.[d]
MDAP	n.d.[d]	n.d.[d]	n.d.[d]	8.5 ± 1.2
H-PLIYLRLLRGQF-OH	0.318 ± 0.038	n.d.[d]	n.d.[d]	n.d.[d]
H-R_7-OH	700 ± 340	287 ± 99	n.b.[c]	n.b.[c]
H-LRRWSLG-OH	1.06 ± 0.17	1.02 ± 0.11	n.b.[c]	n.b.[c]
H-LRRWpSLG-OH	0.0495 ± 0.0034	0.148 ± 0.018	n.b.[c]	n.b.[c]
H-WKRTLRRL-OH	11.8 ± 1.2	27.9 ± 4.8	0.414 ± 0.034	4.29 ± 0.41
H-WKRpTLRRL-OH	0.418 ± 0.068	1.22 ± 0.09	0.407 ± 0.025	4.06 ± 0.55
H-FR_7-OH	44.0 ± 16.8	12.4 ± 3.4	294.0 ± 91	20.2 ± 0.4

[a] in 10 mM Hepes, pH 7.0. [b] in 10 mM $(NH_4)_2HPO_4$, pH 7.0. [c] n.b. = no binding. [d] n.d. = not determined.

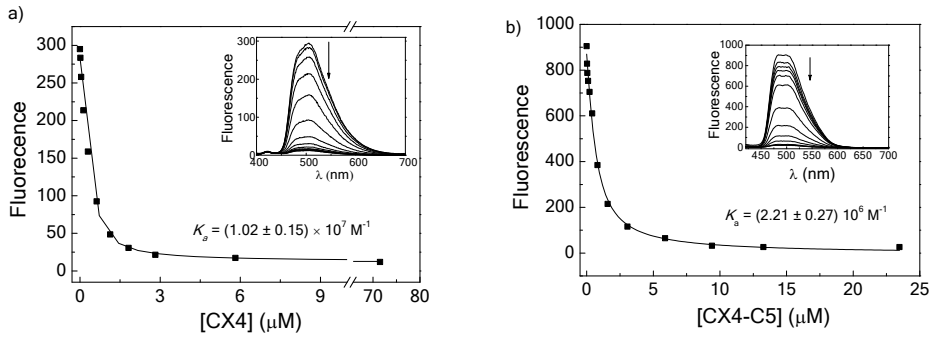

Figure S1. Determination of association constants of a) CX4 and b) CX4-C5 with LCG (0.5 μM) in 10 mM Hepes, pH 7.0 by fluorescence titrations (λ_{ex}= 369 nm, λ_{em}= 502 nm). The insets show the respective fluorescence spectra.

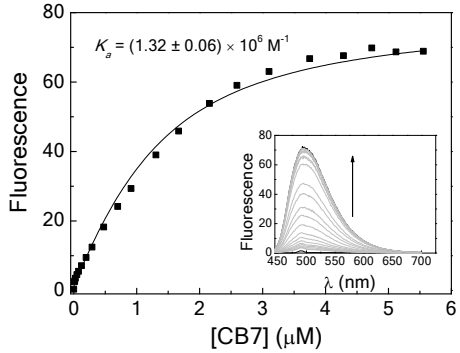

Figure S2. Determination of association constant of CB7 with BE (1 μM) in 10 mM $(NH_4)_2HPO_4$, pH 7.0 by fluorescence titration (λ_{ex}= 420 nm, λ_{em}= 495 nm). The inset shows the respective fluorescence spectra.

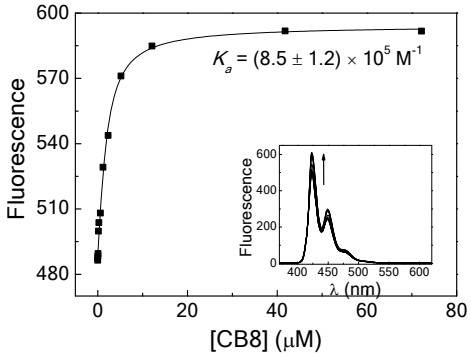

Figure S3. Determination of association constant of CB8 with MDAP (2 μM) in 10 mM Hepes, pH 7.0 by fluorescence titration (λ_{ex}= 339nm, λ_{em}= 424 nm). The inset shows the respective fluorescence spectra.

5 Silently–Translocating Peptide

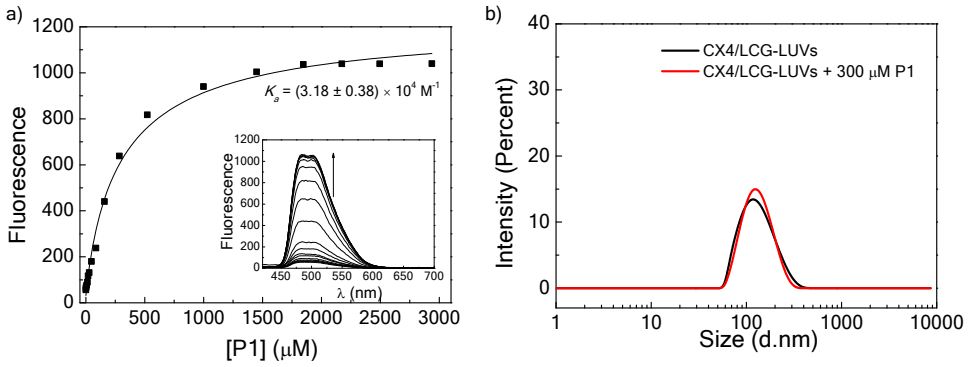

Figure S4. a) Competitive fluorescence titration (λ_{ex}= 369 nm, λ_{em}= 502 nm) with LCG (0.5 μM) to determine the binding constant of **P1** to CX4 (1 μM) in 10 mM Hepes, pH 7.0. The insets show the respective fluorescence spectra. b) Dynamic light scattering of CX4/LCG-LUVs before (black line) and after (red line) addition of **P1** confirming the translocation process without disrupting the LUVs.

6 Identification of Counterion Activators

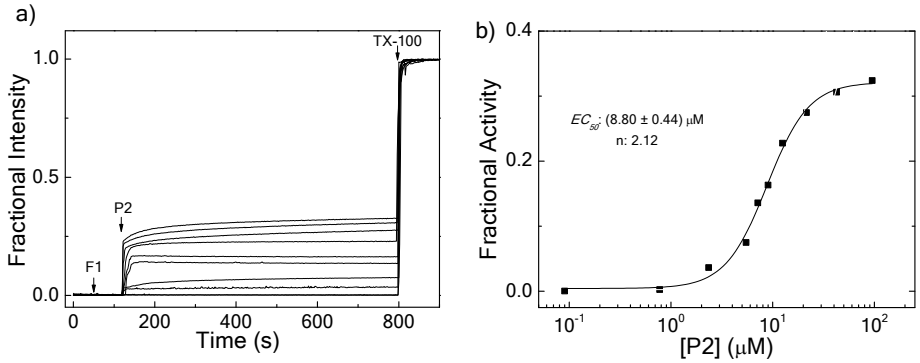

Figure S5. Peptide transport activity. a) Changes in the fractional LCG emission intensity (λ_{ex}= 369 nm, λ_{em}= 502 nm) of POPC⊃CX4/LCG (12 μM phospholipids in 10 mM Hepes, pH 7.0) during the addition of 0.8 μM **F1**, varying concentrations of **P2** (0 – 96 μM), and TX-100 (for calibration). b) Resulting Hill plot analysis.

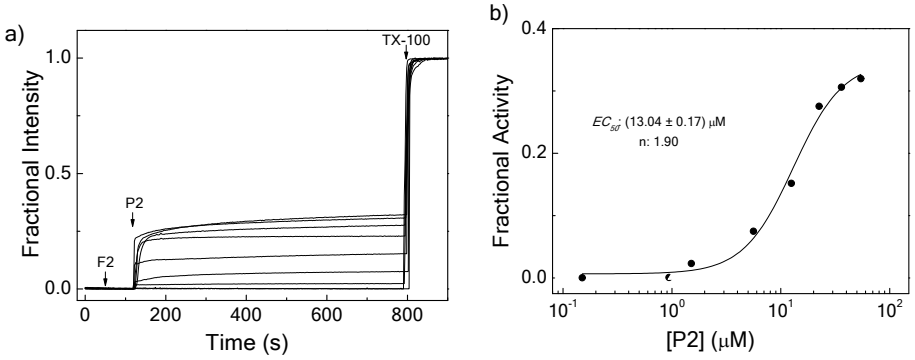

Figure S6. Peptide transport activity. a) Changes in the fractional LCG emission intensity (λ_{ex}= 369 nm, λ_{em}= 502 nm) of POPC⊃CX4/LCG (12 μM phospholipids in 10 mM Hepes, pH 7.0) during the addition of 0.8 μM **F2**, varying concentrations of **P2** (0 – 55 μM), and TX-100 (for calibration). b) Resulting Hill plot analysis.

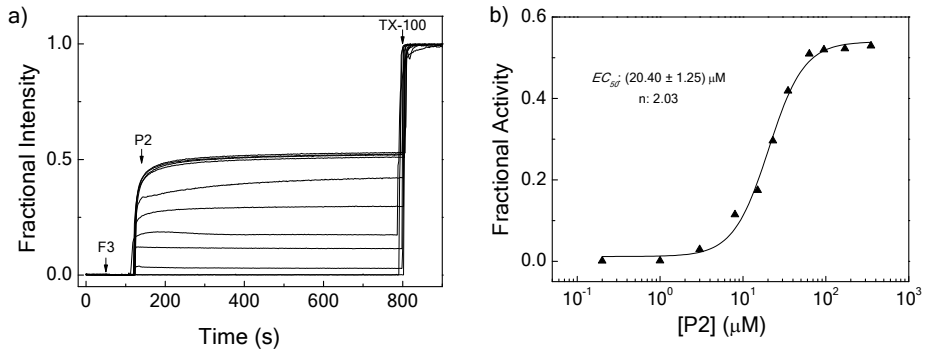

Figure S7. Peptide transport activity. a) Changes in the fractional LCG emission intensity (λ_{ex}= 369 nm, λ_{em}= 502 nm) of POPC⊃CX4/LCG (12 µM phospholipids in 10 mM Hepes, pH 7.0) during the addition of 0.8 µM **F3**, varying concentrations of **P2** (0 – 350 µM), and TX-100 (for calibration). b) Resulting Hill plot analysis.

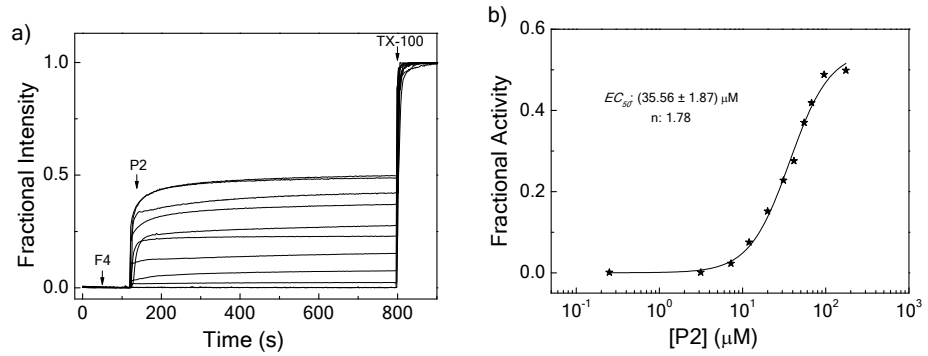

Figure S8. Peptide transport activity. a) Changes in the fractional LCG emission intensity (λ_{ex}= 369 nm, λ_{em}= 502 nm) of POPC⊃CX4/LCG (12 µM phospholipids in 10 mM Hepes, pH 7.0) during the addition of 0.8 µM **F4**, varying concentrations of **P2** (0 – 175 µM), and TX-100 (for calibration). b) Resulting Hill plot analysis.

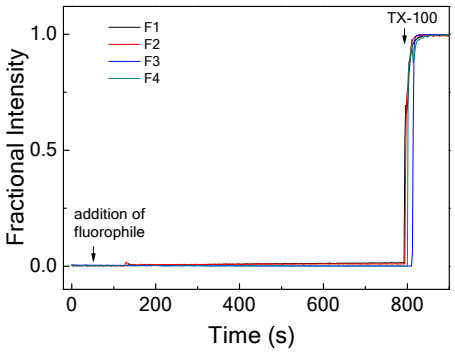

Figure S9. Fractional LCG emission intensity (λ_{ex}= 369 nm, λ_{em}= 502 nm) of POPC⊃CX4/LCG (12 µM phospholipids in 10 mM Hepes, pH 7.0) after the addition of **F1-4** (0.8 µM) and TX-100 (for calibration).

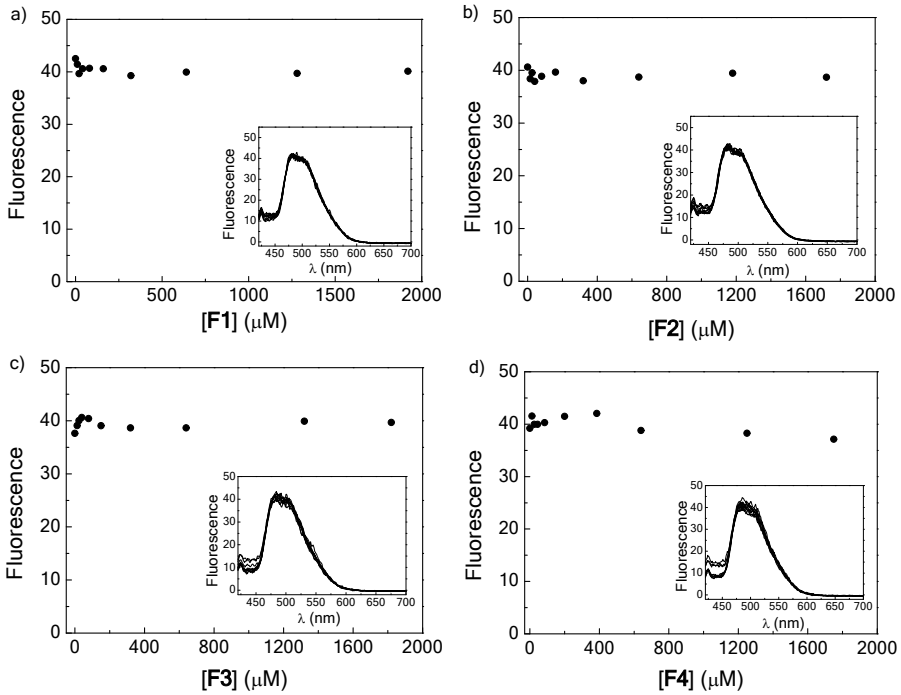

Figure S10. Competitive fluorescence titrations (λ_{ex}= 369 nm, λ_{em}= 502 nm) with LCG (0.5 μM) and CX4 (1 μM) in 10 mM Hepes, pH 7.0 demonstrating that neither a) **F1**, b) **F2**, c) **F3**, nor d) **F4** bind efficiently with CX4.The insets show the respective fluorescence spectra.

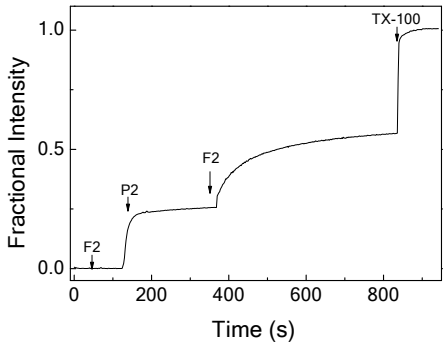

Figure S11. Fractional LCG emission intensity (λ_{ex}= 369 nm, λ_{em}= 502 nm) of POPC⊃CX4/LCG (12 μM phospholipids in 10 mM Hepes, pH 7.0) during the addition of **F2** (0.8 μM), **P2** (20 μM), **F2** (0.8 μM), and TX-100 (for calibration).

Table S2. Membrane transport efficiencies[a] for **P2** with different activators in CX4/LCG[b] assay.

Activator	EC_{50} (μM)	D (%)[c]
F1	8.8 ± 0.5	32
F2	13.0 ± 0.2	32
F3	20.4 ± 1.3	53
F4	36.6 ± 2.8	50

[a] All experiments were performed with 0.8 μM activator. [b] 10 mM Hepes pH 7.0. [c] % Displacement of the dye.

7 Influence of Different Reporter Pairs

7.1 Solution Experiments

7.1.1 Binding of Peptides P2-P7 to CX4-H

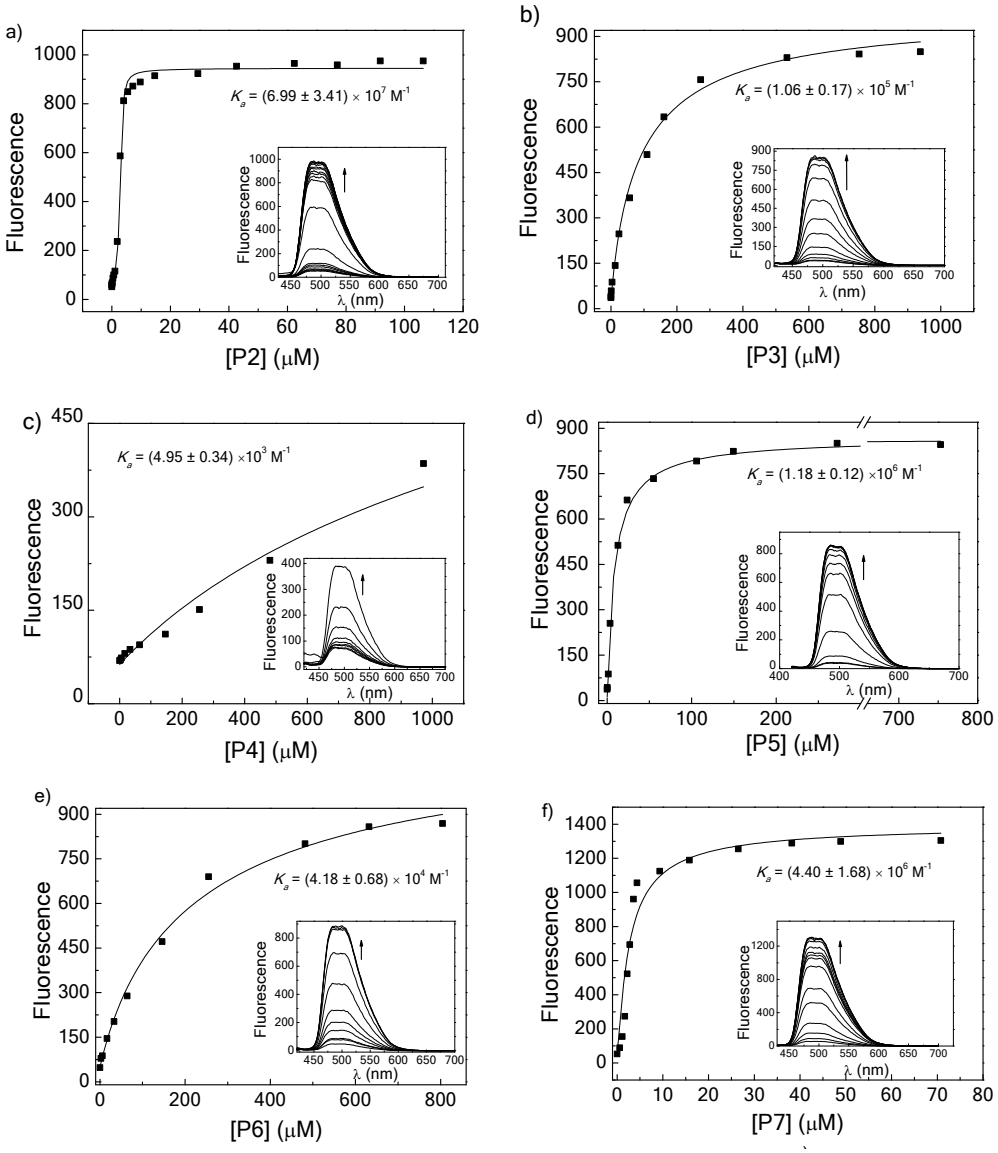

Figure S12. Competitive fluorescence titrations (λ_{ex}= 369 nm, λ_{em}= 502 nm) with LCG (0.5 μM) to determine the binding constants of a) **P2**, b) **P3**, c) **P4**, d) **P5**, e) **P6**, and, f) **P7** to CX4 (1 μM) in 10 mM Hepes, pH 7.0. The insets show the respective fluorescence spectra.

7.1.2 Binding of Peptides P2-P7 2to Curcurbit[7]uril

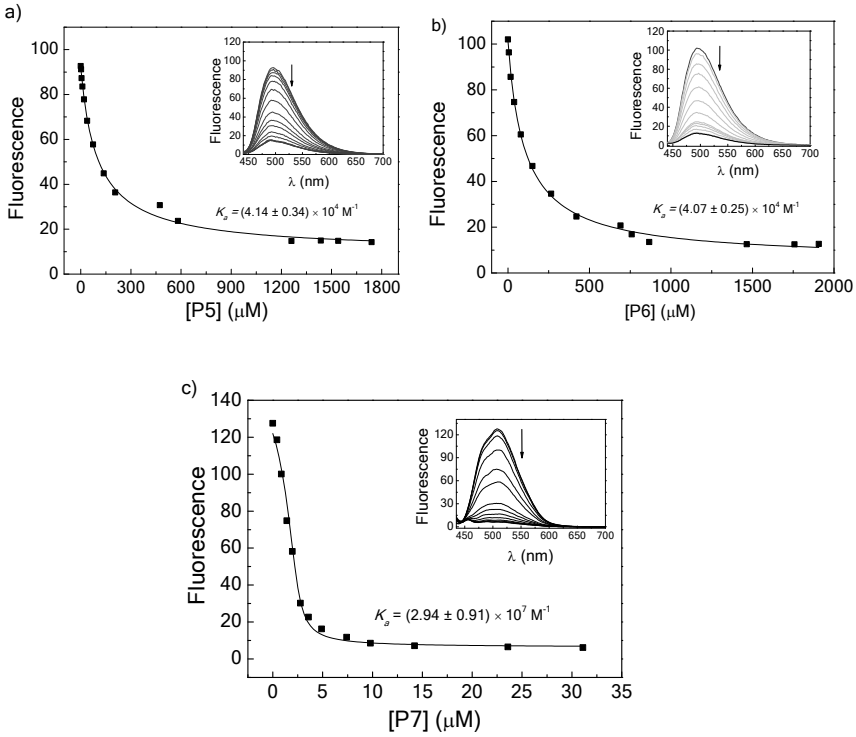

Figure S13. Competitive fluorescence titrations (λ_{ex}= 420 nm, λ_{em}= 495 nm) with BE (1 μM) to determine the binding constants of a) **P5**, b) **P6**, and, c) **P7** to CB7 (2.5 μM) in 10 mM $(NH_4)_2HPO_4$, pH 7.0. The insets show the respective fluorescence spectra.

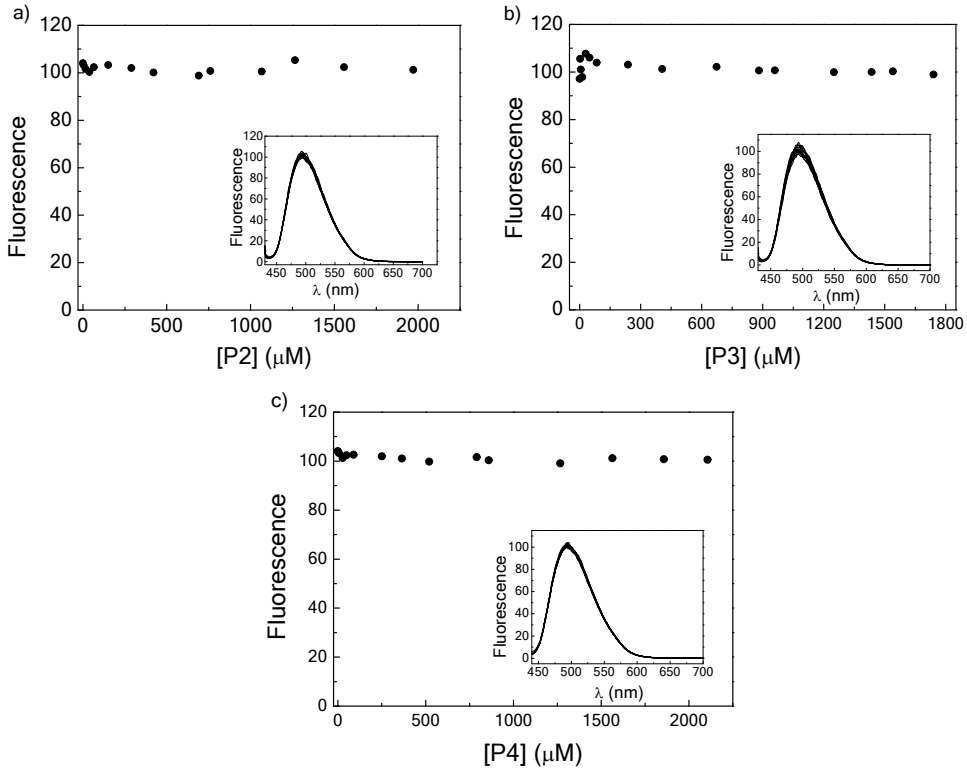

Figure S14. Competitive fluorescence titrations (λ_{ex}= 420 nm, λ_{em}= 495 nm) with BE (1 μM) and CB7 (2.5 μM) in 10 mM $(NH_4)_2HPO_4$, pH 7.0, demonstrating that neither a) **P2**, b) **P3**, nor c) **P4** bind efficiently with CB7. The insets show the respective fluorescence spectra.

7.1.3 Binding of Peptides P2-P7 to Curcurbit[8]uril/MDAP

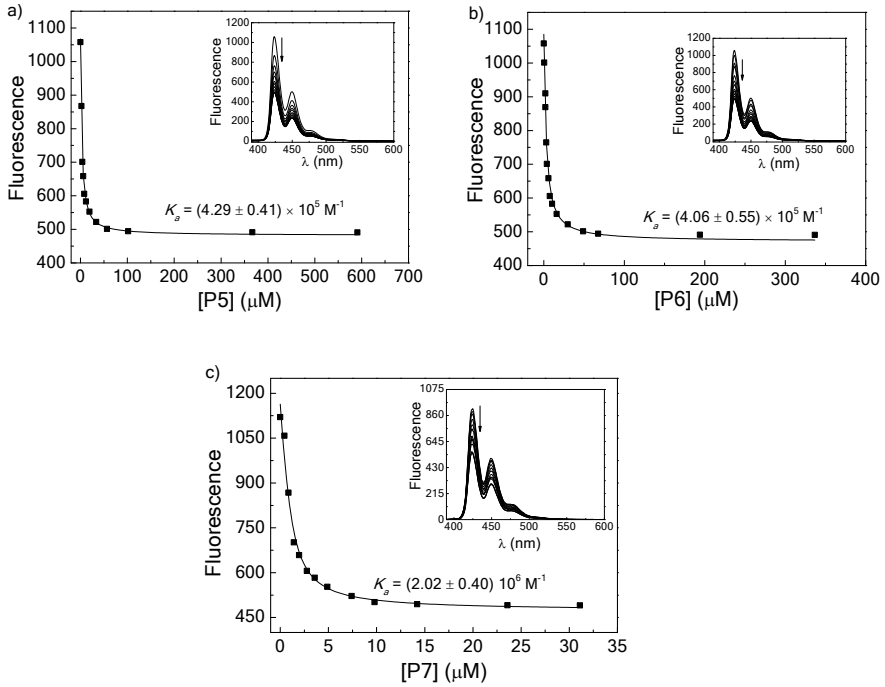

Figure S15. Fluorescence titrations (λ_{ex} = 339 nm, λ_{em} = 420 nm) with CB8 (1 μM) and MDAP (1 μM) to determine the binding constants of a) **P5**, b) **P6**, and, c) **P7** to CB8 (1 μM) in 10 mM Hepes, pH 7.0. The insets show the respective fluorescence spectra.

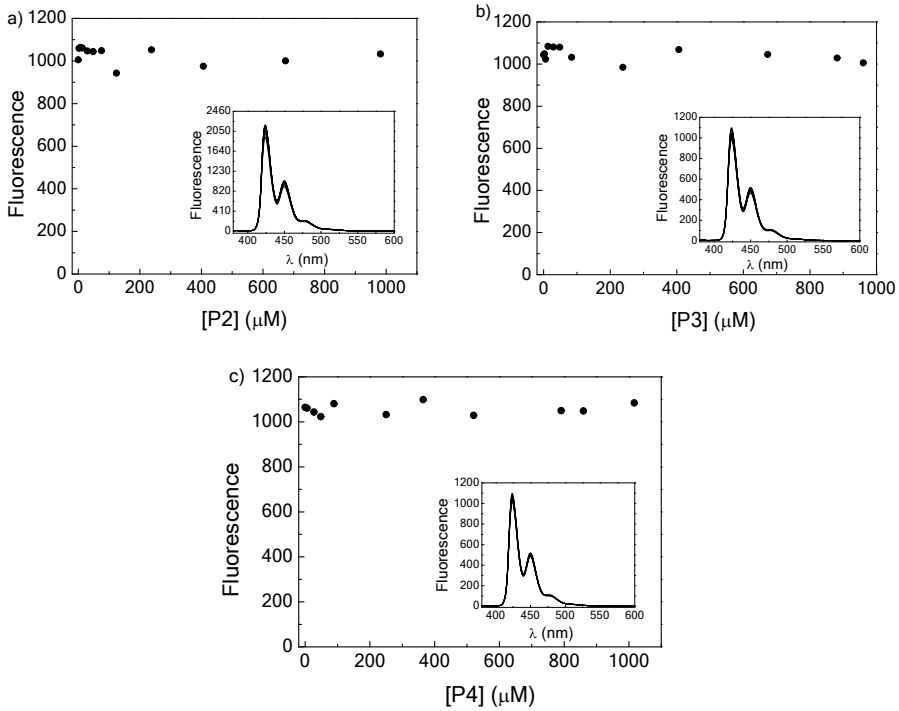

Figure S16. Competitive fluorescence titrations (λ_{ex} = 339 nm, λ_{em} = 424 nm) with CB8 (1 μM) and MDAP (1 μM) in 10 mM Hepes, pH 7.0 demonstrating that neither a) **P2**, b) **P3**, nor c) **P4** bind efficiently with CB8. The insets show the respective fluorescence spectra.

7.1.4 Binding of Peptides P2-P7 to CX4-C5

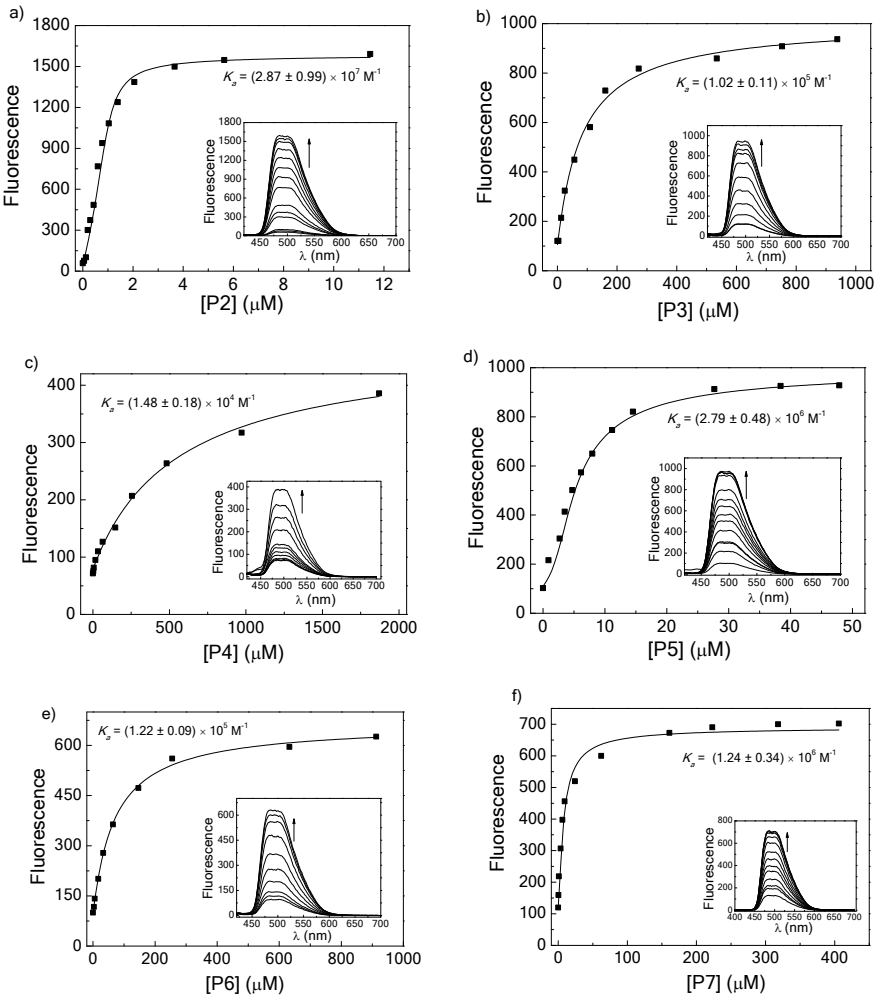

Figure S17. Competitive fluorescence titrations (λ_{ex} = 369 nm, λ_{em} = 502 nm) with LCG (0.5 μM) to determine the binding constants of a) **P2**, b) **P3**, c) **P4**, d) **P5**, e) **P6**, and f) **P7** to CX4-C5 (3.5 μM) in 10 mM Hepes, pH 7.0. The insets show the respective fluorescence spectra.

7.2 Membrane Transport Experiments

7.2.1 CX4/LGC Assay

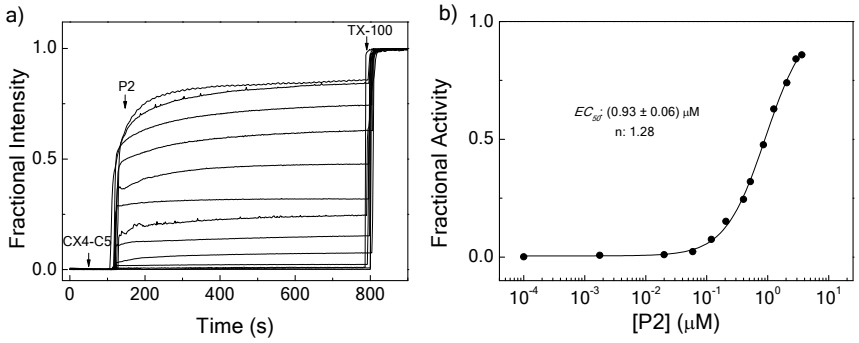

Figure S18. Peptide transport activity. a) Changes in the fractional LCG emission intensity (λ_{ex} = 369 nm, λ_{em} = 502 nm) of POPC⊃CX4/LCG (12 μM phospholipids in 10 mM Hepes, pH 7.0) during the addition of 0.8 μM **CX4-C5**, varying concentrations of **P2** (0 - 4 μM), and TX-100 (for calibration). b) Resulting Hill plot analysis.

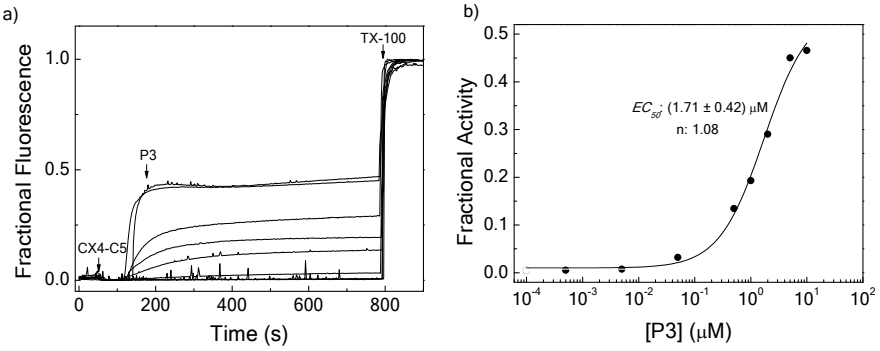

Figure S19. Peptide transport activity. a) Changes in the fractional LCG emission intensity (λ_{ex} = 369 nm, λ_{em} = 502 nm) of POPC⊃CX4/LCG (12 μM phospholipids in 10 mM Hepes, pH 7.0) during the addition of 0.8 μM **CX4-C5**, varying concentrations of **P3** (0 - 10 μM), and TX-100 (for calibration). b) Resulting Hill plot analysis.

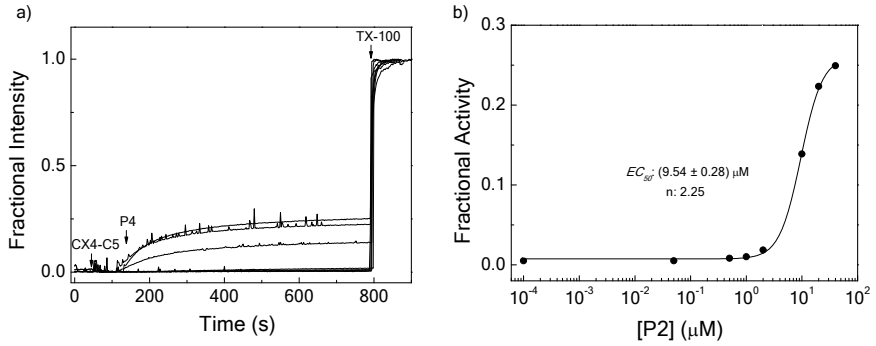

Figure S20. Peptide transport activity. a) Changes in the fractional LCG emission intensity (λ_{ex} = 369 nm, λ_{em} = 502 nm) of POPC⊃CX4/LCG (12 μM phospholipids in 10 mM Hepes, pH 7.0) during the addition of 0.8 μM **CX4-C5**, varying concentrations of **P4** (0 - 40 μM), and TX-100 (for calibration). b) Resulting Hill plot analysis.

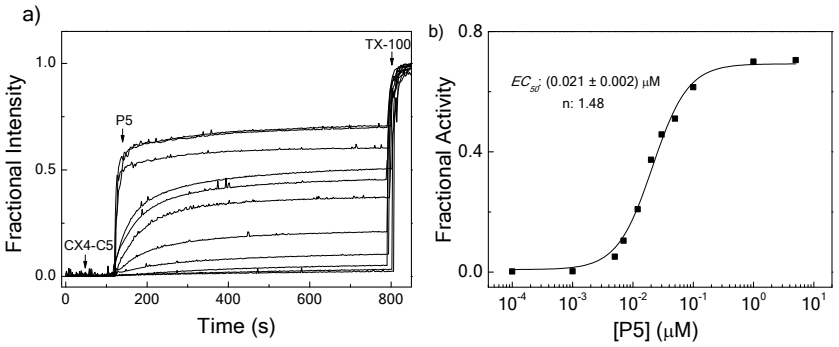

Figure S21. Peptide transport activity. a) Changes in the fractional LCG emission intensity (λ_{ex} = 369 nm, λ_{em} = 502 nm) of POPC⊃CX4/LCG (12 μM phospholipids in 10 mM Hepes, pH 7.0) during the addition of 0.8 μM **CX4-C5**, varying concentrations of **P5** (0 - 5 μM), and TX-100 (for calibration). b) Resulting Hill plot analysis.

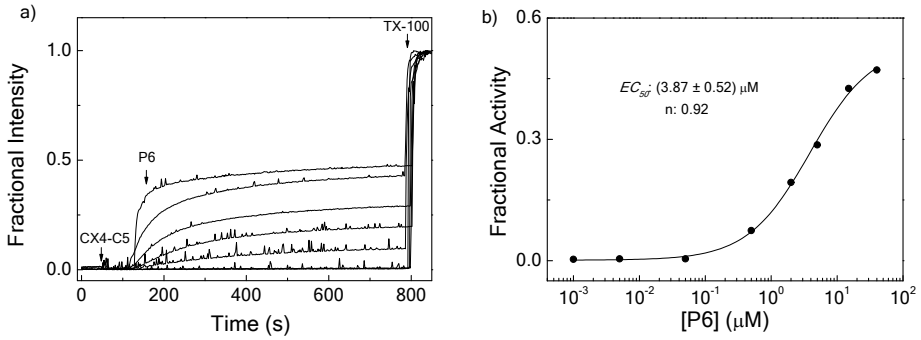

Figure S22. Peptide transport activity. a) Changes in the fractional LCG emission intensity (λ_{ex} = 369 nm, λ_{em} = 502 nm) of POPC⊃CX4/LCG (12 μM phospholipids in 10 mM Hepes, pH 7.0) during the addition of 0.8 μM **CX4-C5**, varying concentrations of **P6** (0 - 40 μM), and TX-100 (for calibration). b) Resulting Hill plot analysis.

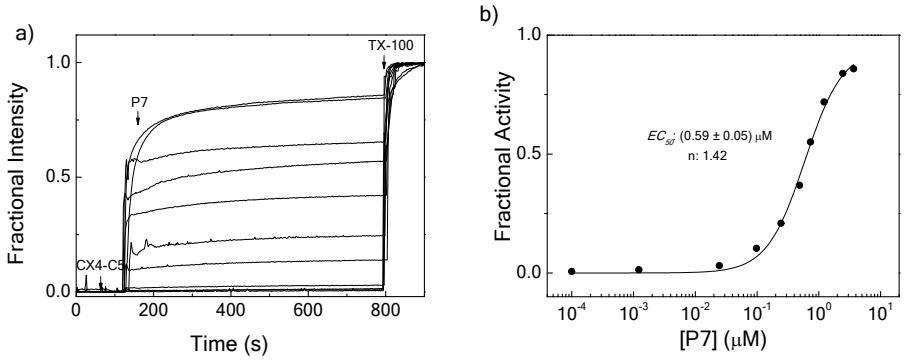

Figure S23. Peptide transport activity. a) Changes in the fractional LCG emission intensity (λ_{ex} = 369 nm, λ_{em} = 502 nm) of POPC⊃CX4/LCG (12 μM phospholipids in 10 mM Hepes, pH 7.0) during the addition of 0.8 μM **CX4-C5**, varying concentrations of **P7** (0 - 4 μM), and TX-100 (for calibration). b) Resulting Hill plot analysis.

7.2.2 CB7/BE Assay

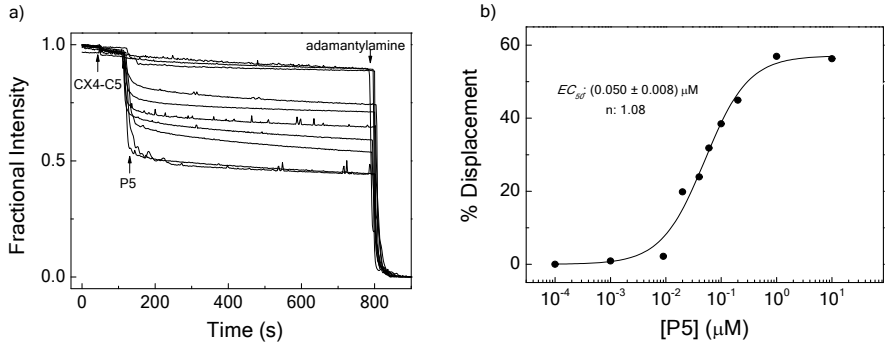

Figure S24. Peptide transport activity. a) Changes in the fractional BE emission intensity (λ_{ex} = 420 nm, λ_{em} = 495 nm) of POPC/POPS⊃CB7/BE (12 μM phospholipids in 10 mM $(NH_4)_2HPO_4$, pH 7.0) during the addition of 0.8 μM **CX4-C5**, varying concentrations of **P5** (0 - 10 μM), and 25 μM of adamantylamine (for calibration). b) Resulting Hill plot analysis.

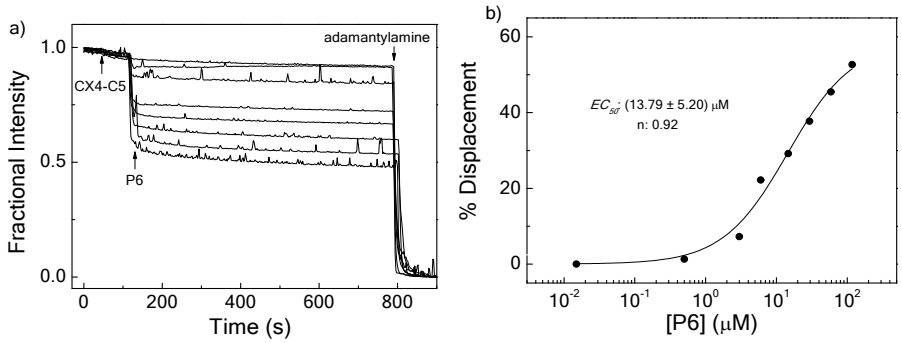

Figure S25. Peptide transport activity. a) Changes in the fractional BE emission intensity (λ_{ex} = 420 nm, λ_{em} = 495 nm) of POPC/POPS⊃CB7/BE (12 μM phospholipids in 10 mM $(NH_4)_2HPO_4$, pH 7.0) during the addition of 0.8 μM **CX4-C5**, varying concentrations of **P6** (0 - 120 μM), and 25 μM of adamantylamine (for calibration). b) Resulting Hill plot analysis.

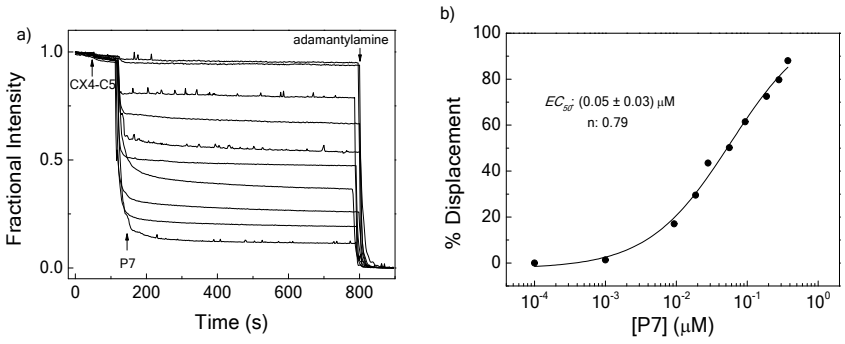

Figure S26. Peptide transport activity. a) Changes in the fractional BE emission intensity (λ_{ex} = 420 nm, λ_{em} = 495 nm) of POPC/POPS⊃CB7/BE (12 μM phospholipids in 10 mM $(NH_4)_2HPO_4$, pH 7.0) during the addition of 0.8 μM **CX4-C5**, varying concentrations of **P7** (0 – 0.4 μM), and 25 μM of adamantylamine (for calibration). b) Resulting Hill plot analysis.

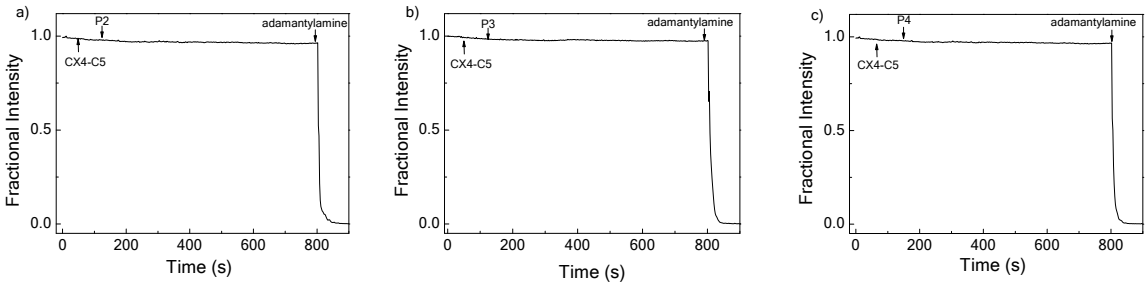

Figure S27: Fractional BE emission intensity (λ_{ex} = 420 nm; λ_{em} = 495 nm) of POPC/POPS⊃CB7/BE (12 µM phospholipids in 10 mM $(NH_4)_2HPO_4$, pH 7.0) during the addition of 0.8 µM **CX4-C5**, a) **P2** (10 µM), or b) **P3** (10 µM), or c) **P4** (10 µM), and adamantylamine (for calibration).

7.2.3 CB8/MDAP Assay

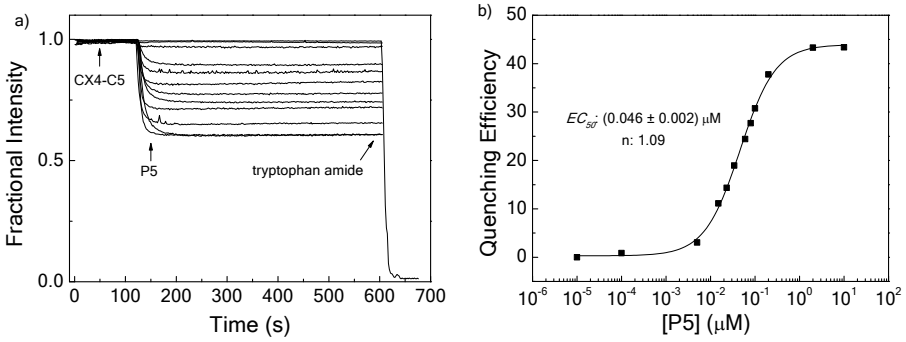

Figure S28. Peptide transport activity. a) Changes in the fractional MDAP emission intensity (λ_{ex} = 339 nm, λ_{em} = 424 nm) of POPC/POPS⊃CB8/MDAP (12 µM phospholipids in 10 mM Hepes, pH 7.0) during the addition of 0.8 µM **CX4-C5**, varying concentrations of **P5** (0 - 10 µM), and 25 µM tryptophan amide (for calibration). b) Resulting Hill plot analysis.

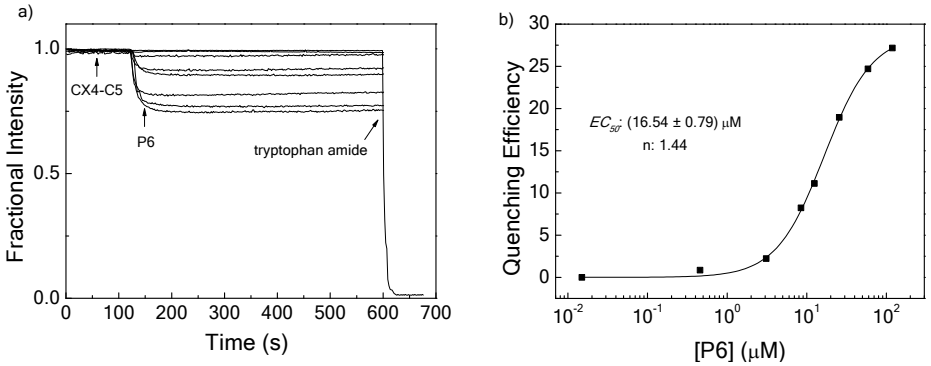

Figure S29. Peptide transport activity. a) Changes in the fractional MDAP emission intensity (λ_{ex} = 339 nm, λ_{em} = 424 nm) of POPC/POPS⊃CB8/MDAP (12 µM phospholipids in 10 mM Hepes, pH 7.0) during the addition of 0.8 µM **CX4-C5**, varying concentrations of **P6** (0 - 120 µM), and 25 µM tryptophan amide (for calibration). b) Resulting Hill plot analysis.

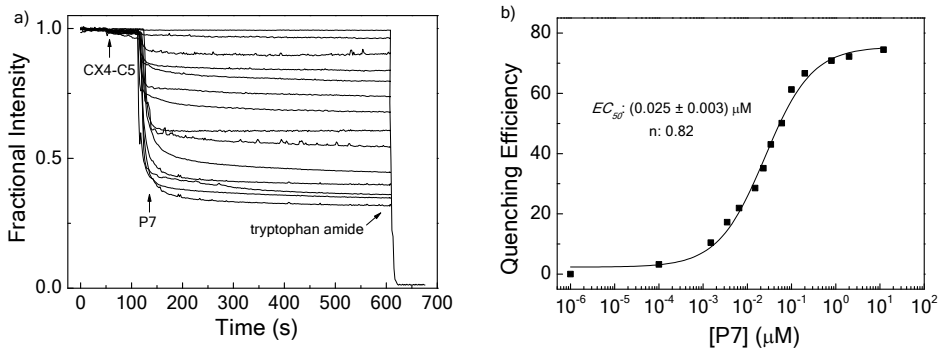

Figure S30. Peptide transport activity. a) Changes in the fractional MDAP emission intensity (λ_{ex} = 339 nm, λ_{em} = 424 nm) of POPC/POPS⊃CB8/MDAP (12 μM phospholipids in 10 mM Hepes, pH 7.0) during the addition of 0.8 μM **CX4-C5**, varying concentrations of **P7** (0 - 12 μM), and 25 μM tryptophan amide (for calibration). b) Resulting Hill plot analysis.

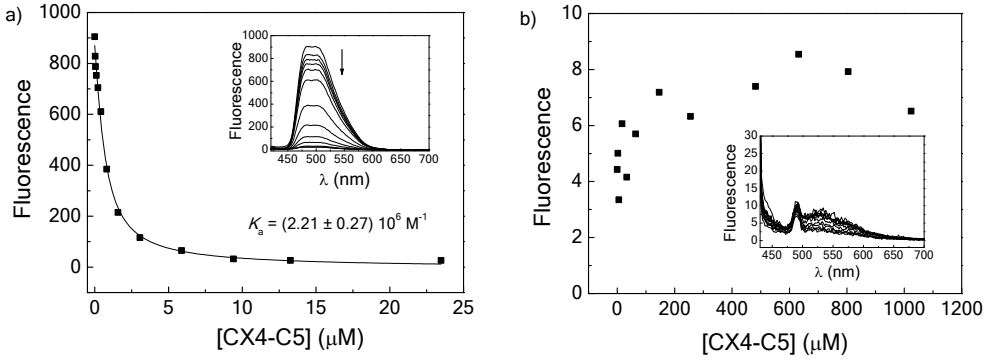

Figure S31. a) Determination of association constant of CX4-C5 with LCG (0.5 μM) in 10 mM Hepes, pH 7.0 by fluorescence titration (λ_{ex} = 369 nm, λ_{em} = 502 nm). b) Fluorescence titration (λ_{ex} = 420 nm, λ_{em} = 495 nm) of BE (1 μM) with **CX4-C5** in 10 mM $(NH_4)_2HPO_4$, pH 7.0 demonstrating that BE does not bind efficiently with **CX4-C5**. The insets show the respective fluorescence spectra.

8 Transport in GUVs

8.1 CB8/MDAP Assay

The principle of monitoring peptide uptake into vesicles by means of an encapsulated CB7/BE reporter pair is shown in Scheme S3 on page S6. To prepare POPC/POPS (9/1) GUVs by electroformation,[S8,S9] 30 µL POPC solution (25 mg/mL in $CHCl_3$) and 10 µL POPS solution (10 mg/mL in $CHCl_3$) were spread on ITO-coated glass slide. After the solvent was evaporated, the dried film was rehydrated with 300 mM sucrose solution containing 500 µM CB8 and 550 µM MDAP and covered with another ITO slide. Electroformation proceeded at 3.0 V, 5 Hz, at 37˚C for 2 h in Vesicle Prep Pro.

Fluorescence microscopy of GUVs was performed with an Axiovert 200 (Carl Zeiss, filter set 02, i.e., G365 nm, FT 395 nm and BP 420 nm) equipped with a digital camera (Evolution QEi monochrome) through a 20x objective on samples prepared by adding 10 µL of GUV suspension on a glass slide. The analysis of the images was performed in ImageJ software by measuring the average intensity of an area corresponding to one GUV for the series of time-lapsed images.

8.1.1 Peptide Activation with Fluorophiles

In a typical experiment, first, 5 µM of non-permeating analyte tryptophan was added to the GUV suspension to saturate the non-encapsulated reporter pair and quench the extravesicular emission; then, 0.8 µM of amphiphilic activator (**F1, F2, F3**, or **F4**), and finally, 10 µM of **P7** were added. Images were taken at regular intervals (60 s) thereafter. The sample was irradiated only when the images where taken in order to avoid possible photobleaching.

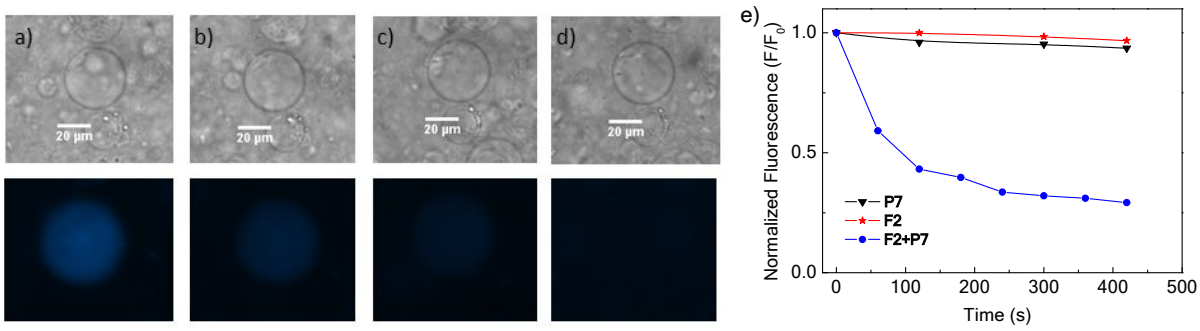

Figure S32. Bright-field (top) and fluorescence (bottom) microscopy images after the addition of tryptophan (5 µM), then **F2** (0.8 µM), and finally, **P7** (10 µM) a) after 0 s, b) 60 s, c) 300 s, and d) 420 s. e) Normalized fluorescence intensities of GUVs monitored at different times (blue circles). No significant change in fluorescence was observed with **P7** (black triangles) or **F2** (red stars) only.

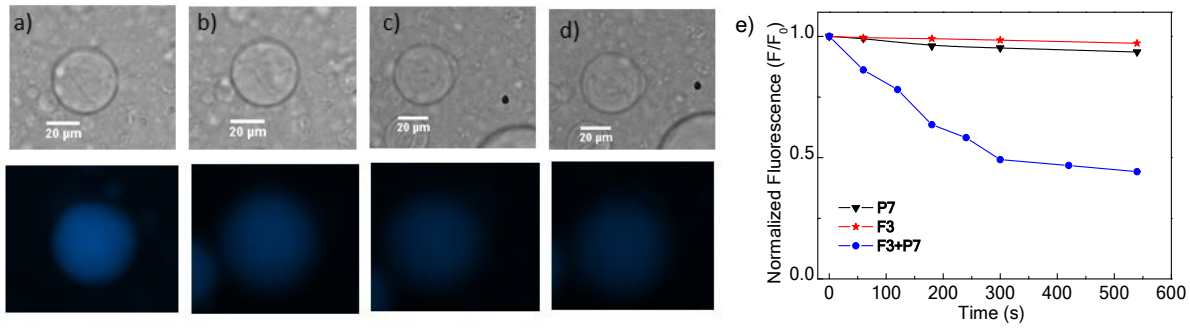

Figure S33. Bright-field (top) and fluorescence (bottom) microscopy images after the addition of tryptophan (5 µM), then **F3** (0.8 µM), and finally, **P7** (10 µM) a) after 0 s, b) 120 s, c) 300 s, and d) 540 s. e) Normalized fluorescence intensities of GUVs monitored at different times (blue circles). No significant change in fluorescence was observed with **P7** (black triangles) or **F3** (red stars) only.

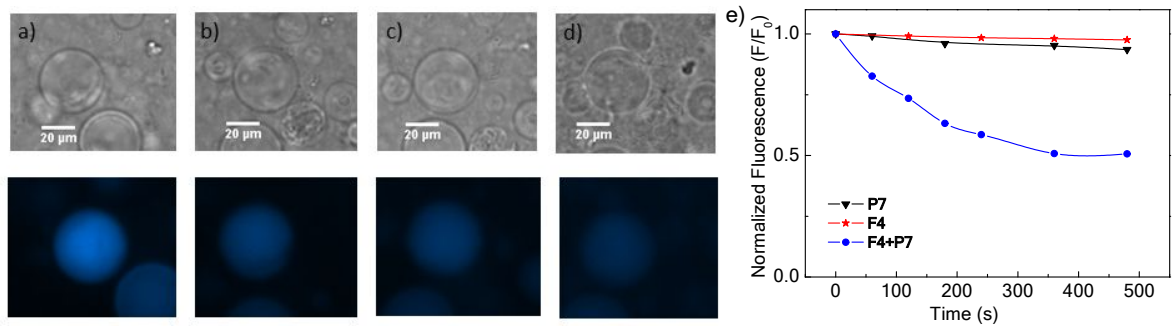

Figure S34. Bright-field (top) and fluorescence (bottom) microscopy images after the addition of tryptophan (5 µM), then **F4** (0.8 µM), and finally, **P7** (10 µM) a) after 0 s, b) 60 s, c) 240 s, and d) 480 s. e) Normalized fluorescence intensities of GUVs monitored at different times (blue circles). No significant change in fluorescence was observed with **P7** (black triangles) or **F4** (red stars) only.

8.1.2 Peptide Activation with CX4-C5

In a typical experiment, first, 5 µM of non-permeating analyte tryptophan was added to the GUV suspension to saturate the non-encapsulated reporter pair and quench the extravesicular emission; then, 0.8 µM of amphiphilic activator **CX4-C5**, and finally, 10 µM of peptide (**P5**, **P6**, or **P7**) were added. Images were taken at regular intervals (60 s) thereafter. The sample was irradiated only when the images where taken in order to avoid possible photobleaching.

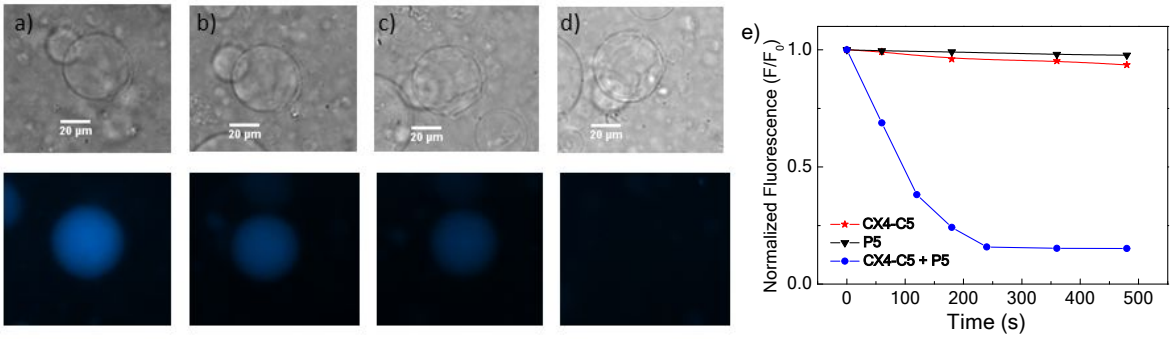

Figure S35. Bright-field (top) and fluorescence (bottom) microscopy images after the addition of tryptophan (5 µM), then **CX4-C5** (0.8 µM), and finally, **P5** (10 µM) a) after 0 s, b) 60 s, c) 180 s, and d) 480 s. e) Normalized fluorescence intensities of GUVs monitored at different times (blue circles). No significant change in fluorescence was observed with **CX4-C5** (red stars) or **P5** (black triangles) only.

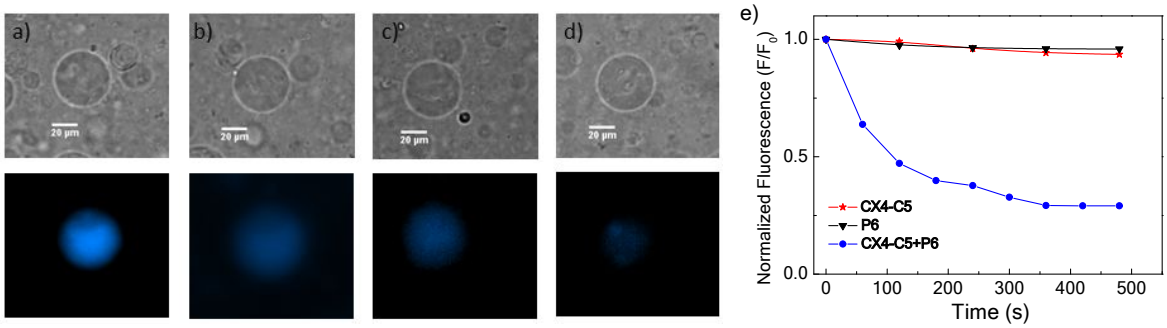

Figure S36. Bright-field (top) and fluorescence (bottom) microscopy images after the addition of tryptophan (5 µM), then **CX4-C5** (0.8 µM), and finally, **P6** (10 µM) a) after 0 s, b) 120 s, c) 360 s, and d) 480 s. e) Normalized fluorescence intensities of GUVs monitored at different times (blue circles). No significant change in fluorescence was observed with **CX4-C5** (red stars) or **P6** (black triangles) only.

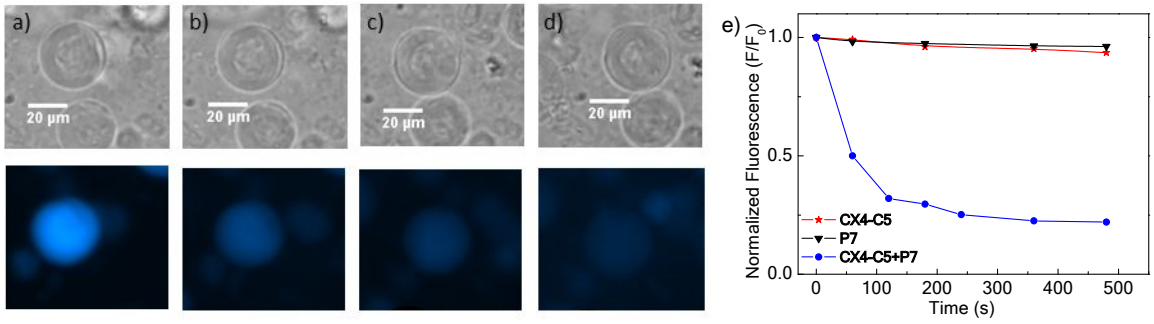

Figure S37. Bright-field (top) and fluorescence (bottom) microscopy images after the addition of tryptophan (5 µM), then **CX4-C5** (0.8 µM), and finally, **P7** (10 µM) a) after 0 s, b) 60 s, c) 180 s, and d) 480 s. e) Normalized fluorescence intensities of GUVs monitored at different times (blue circles). No significant change in fluorescence was observed with **CX4-C5** (red stars) or **P7** (black triangles) only.

8.2 CX4/LCG Assay

The principle of monitoring peptide uptake into vesicles by means of an encapsulated LCG/CX reporter pair is shown in Scheme S1 on page S3. POPC GUVs were prepared by electroformation.[S8,S9] Briefly, 30 µL POPC solution (25 mg/mL in $CHCl_3$) was spread on an ITO-coated glass slide. After the solvent was evaporated, the dried film was rehydrated with 275 µL 300 mM sucrose solution containing 700 µM CX4 and 500 µM LCG and covered with another ITO slide. Electroformation proceeded at 3.0 V, 5 Hz, at 37 ˚C for 2 h in Vesicle Prep Pro. Extravesicular reporter pair was removed by transferring the GUV suspension into a cellulose dialysis bag (typical MWCO = 14 kDa) and dialysing it twice for 1 h with 500 mL 300 mM sucrose.

Fluorescence microscopy of GUVs was performed with an Axiovert 200 (Carl Zeiss, filter set 02, i.e., G365 nm, FT 395 nm and BP 420 nm) equipped with a digital camera (Evolution QEi monochrome) through a 20x objective on samples prepared by adding 10 µL of GUV suspension on a glass slide. The analysis of the images was performed in ImageJ software by measuring the average intensity of an area corresponding to one GUV for the series of time-lapsed images.

8.2.1 Previously Silently Translocating Peptide

For transport experiment 20 µM of **P1** were added to the GUVs suspension and images were taken at regular intervals (60 s) thereafter. The sample was irradiated only when the images where taken in order to avoid possible photobleaching.

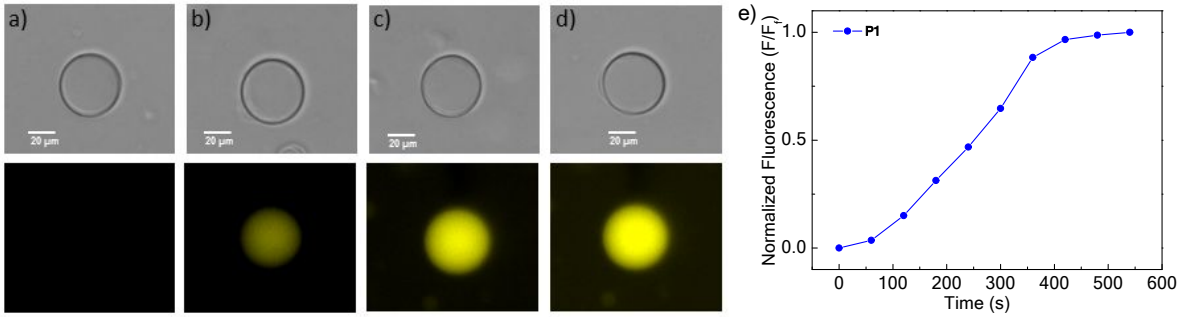

Figure S38. Bright-field (top) and fluorescence (bottom) microscopy images after the addition of **P1** (20 µM) a) after 0 s, b) 120 s, c) 360 s, and d) 540 s. e) Normalized fluorescence intensities of GUVs monitored at different times.

8.2.2 Heptaarginine Activation with CX4-C5

For transport experiment 0.8 µM of **CX4-C5** and 20 µM of **P2** were added to the GUVs suspension and images were taken at regular intervals (60 s) thereafter. The sample was irradiated only when the images where taken in order to avoid possible photobleaching.

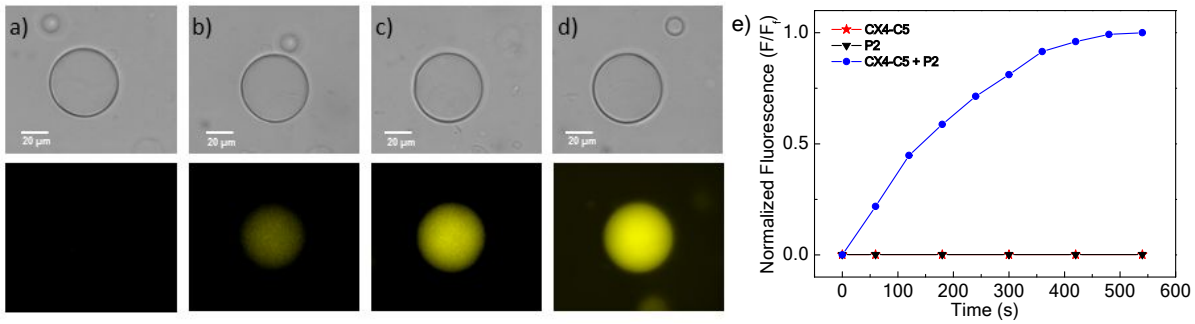

Figure S39. Bright-field (top) and fluorescence (bottom) microscopy images after the addition of **CX4-C5** (0.8 µM), and **P2** (20 µM) a) after 0 s, b) 60 s, c) 180 s, and d) 420 s. e) Normalized fluorescence intensities of GUVs monitored at different times (blue circles). No change in fluorescence was observed with **CX4-C5** (red stars) or **P2** (black triangles) only.

8.2.3 LCG Photobleaching

The fluorescence of GUVs containing only LCG was monitored over time without any compound addition to estimate the effect of photobleaching. After 10 min continuous irradiation the photobleaching was ≈ 10%, in line with previously reported values[S10,S11]. This 10% bleaching could be considered insignificant compared with the increase in fluorescence obtained in the transport experiments.

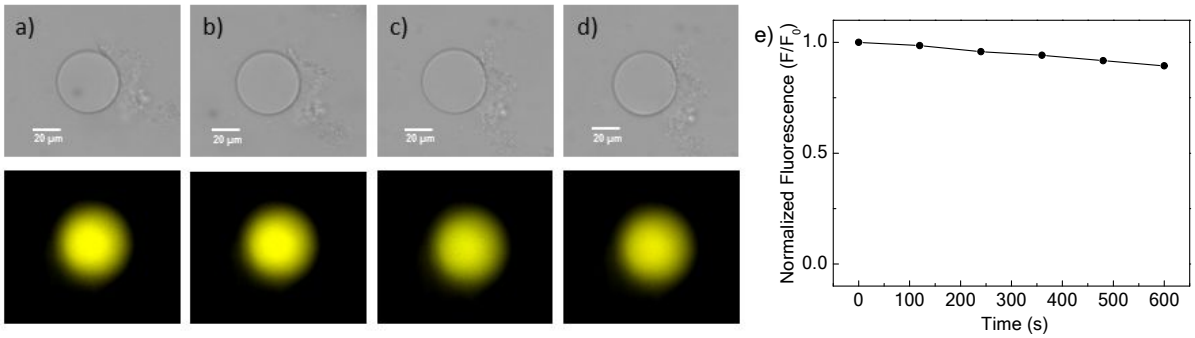

Figure S40. Bright-field (top) and fluorescence (bottom) microscopy images a) at the beginning of the experiment (0 s), and after b) 120 s, c) 360 s, and d) 600 s irradiation time to quantify lucigenin photobleaching. e) Normalized fluorescence intensities of GUVs monitored after different irradiation times.

9 References

(S1) Blacker, A. J.; Jazwinski, J.; Lehn, J.-M., Molecular Anion Binding and Substrate Photooxidation in Visible Light by 2,7-Diazapyrenium Cations. *Helv. Chim. Acta* **1987**, *70*, 1-12.
(S2) Peng, S.; Barba-Bon, A.; Pan, Y.-C.; Nau, W. M.; Guo, D.-S.; Hennig, A., Phosphorylation-Responsive Membrane Transport of Peptides. *Angew. Chem. Int. Ed.* **2017**, *56*, 15742-15745.
(S3) Mach, H.; Middaugh, C. R.; Lewis, R. V., Statistical determination of the average values of the extinction coefficients of tryptophan and tyrosine in native proteins. *Anal. Biochem.* **1992**, *200*, 74-80.
(S4) Fasman, G. D. In *Handbook of Biochemistry and Molecular Biology*; 3rd Edition ed.; CRC Press Cleveland, Ohio 1976; Vol. I, p 183-203.
(S5) Hein, R.; Uzundal, C. B.; Hennig, A., Simple and rapid quantification of phospholipids for supramolecular membrane transport assays. *Org. Biomol. Chem.* **2016**, *14*, 2182-2185.
(S6) Ghale, G.; Lanctôt, A. G.; Kreissl, H. T.; Jacob, M. H.; Weingart, H.; Winterhalter, M.; Nau, W. M., Chemosensing Ensembles for Monitoring Biomembrane Transport in Real Time. *Angew. Chem. Int. Ed.* **2014**, *53*, 2762-2765.
(S7) Dsouza, R. N.; Pischel, U.; Nau, W. M., Fluorescent Dyes and Their Supramolecular Host/Guest Complexes with Macrocycles in Aqueous Solution. *Chem. Rev.* **2011**, *111*, 7941-7980.
(S8) Angelova, M. I.; Soléau, S.; Méléard, P.; Faucon, F.; Bothorel, P. In *Trends in Colloid and Interface Science VI*; Helm, C., Lösche, M., Möhwald, H., Eds.; Steinkopff: Darmstadt, 1992, p 127-131.
(S9) Apellániz, B.; Nieva, J. L.; Schwille, P.; García-Sáez, A. J., All-or-None versus Graded: Single-Vesicle Analysis Reveals Lipid Composition Effects on Membrane Permeabilization. *Biophys. J.* **2010**, *99*, 3619-3628.
(S10) Valkenier, H.; López Mora, N.; Kros, A.; Davis, A. P., Visualization and Quantification of Transmembrane Ion Transport into Giant Unilamellar Vesicles. *Angew. Chem. Int. Ed.* **2015**, *54*, 2137-2141.
(S11) Mora, N. L.; Bahreman, A.; Valkenier, H.; Li, H.; Sharp, T. H.; Sheppard, D. N.; Davis, A. P.; Kros, A., Targeted anion transporter delivery by coiled-coil driven membrane fusion. *Chem. Sci.* **2016**, *7*, 1768-1772.